

**TRANSIENT OVERVOLTAGES ON ROTARY FLUX COMPRESSOR/  
COMPENSATED PULSED ALTERNATOR WINDINGS**

S. B. Pratap, D. R. Brown, and W. L. Bird

Presented at the  
4th IEEE International Pulsed Power Conference  
Albuquerque, New Mexico  
June 6-8, 1983

Publication No. PN-94  
Center for Electromechanics  
The University of Texas at Austin  
Balcones Research Center  
EME 1.100, Building 133  
Austin, TX 78758-4497  
(512)471-4496

PN 094 Pratap

ERRATA

Page 3, first full paragraph:

"The dashed line in figure 4"

Should be

"The dashed line in **figure 5**"

TRANSIENT OVERVOLTAGES ON ROTARY FLUX COMPRESSOR/  
COMPENSATED PULSED ALTERNATOR WINDINGS

S. B. Pratap, D. R. Brown, and W. L. Bird  
Center for Electromechanics  
The University of Texas at Austin  
Austin, TX 78712

Summary

The voltage distributions in the windings of rotary flux compressors and compensated pulsed alternators (RFC/CPAs) have been analyzed using a distributed parameter circuit model. Voltage distributions in response to step inputs and steady state ac distributions have been analyzed and closed-form expressions have been derived. Comparison between experimental observations and analytical predictions have been made. Knowledge of the voltage distribution is required to minimize stress without sacrificing performance.

Introduction

When RFCs are used to drive flashlamp loads, there are high rates of change of applied voltage when the start-up capacitor is connected across the winding and when the energy stored in an intermediate capacitor is discharged into the load. The voltage gradients induced in the windings due to the application of fast-changing voltages may lead to insulation failure.

The initial voltage distribution in response to a step is analyzed first, using a model which includes only the turn-to-turn and turn-to-ground plane capacitance. The analytical expressions indicate a nonlinear distribution, with about 50 percent of the voltage drop taking place in the first turn of the winding, resulting in high potential gradients. Experimental observations indicate a nonlinear but less severe distribution, since a step voltage is likely to be more severe than the terminal voltage conditions actually encountered.

Steady state ac analysis indicates the presence of resonant frequencies. At these resonant frequencies, sharp potential gradients may exist, not only near the end turns, but at a number of places along the length of the winding. Experimental observations confirm the presence of resonant frequencies.

In order to eliminate nonlinear effects of a magnetic core, the experimental observations were made using a wave-type winding of Litz wire, wound on a plexiglass cylinder having an air core. The ground plane was simulated using an aluminum foil wrapped close along the winding.

Figures 1 and 2 show the mathematical models for the winding for the initial distribution in response to a step and steady state ac analysis, respectively.

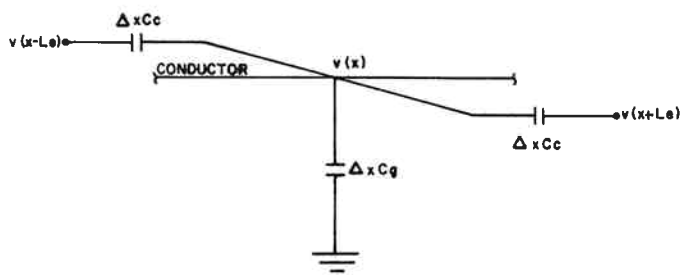


Fig. 1. Circuit model for RFC winding -- step function

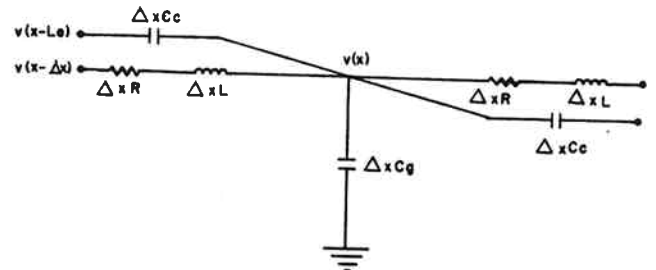


Fig. 2. Circuit model for RFC winding -- steady state

Initial Voltage Distribution  
in Response to a Step

The initial voltage distribution in response to a step is essentially a function of the turn-to-turn and turn-to-ground plane capacitance. The voltage as a function of the winding position can be written as

$$v(x_n) = V_0 \frac{\sinh(n\sqrt{r}(1-x_n))}{\sinh(n\sqrt{r})} \quad (1)$$

where  $r = C_g/C_c$   
 $V_0$  = magnitude of the step voltage  
 $x_n$  = normalized length of the winding  
 $n$  = number of turns.

Figure 3 is the graphical representation of Eq. 1 for three different values of  $C_g/C_c$ . This indicates a higher potential gradient in the first few turns for higher values of  $r$ . Figure 4 shows the experimentally observed voltage distribution for a step voltage. The voltage distribution as observed is nonlinear, but is not as severe as that predicted by Eq. 1. It was observed that as the rate of rise of the applied voltage decreases, the distribution tends to become linear.

From the above, we may conclude that in order to limit the potential gradients across the interturn insulation to safe values, the rate of change of the applied voltage must be low, and the ground capacitance should be minimized.

Steady State AC Voltage Distribution

The steady state ac analysis was done primarily to verify the mathematical model. The observations indicate a good match with the model up to 3 MHz. Beyond this frequency, due to various phenomena associated with higher frequencies that are not accounted for in the model, the match is not perfect.

The steady ac voltage distribution can be written as

$$v(x_n) = V_0 \frac{\sin(\gamma(1-x_n))}{\sin \gamma} \quad \text{for } \omega < 1/(L_e\sqrt{C_c L}) \quad (2)$$

$$v(x_n) = V_0 \frac{\sinh(\gamma(1-x_n))}{\sinh \gamma} \quad \text{for } \omega > 1/(L_e\sqrt{C_c L}) \quad (3)$$

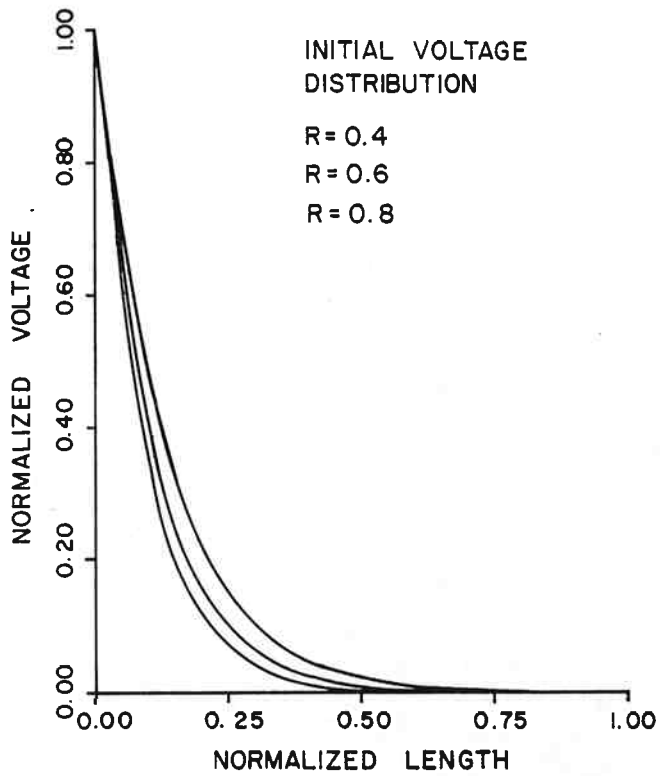


Fig. 3. Initial voltage distribution

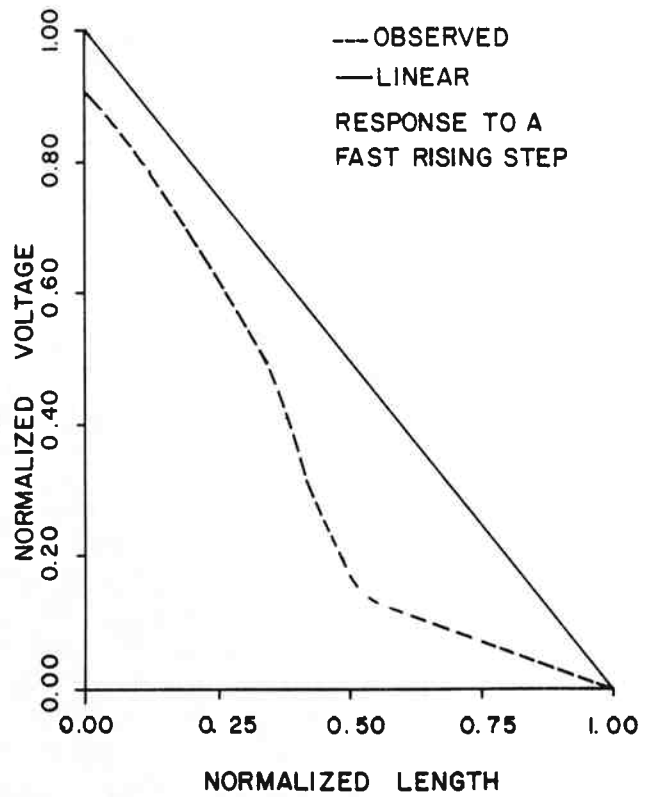


Fig. 4. Response to a step voltage

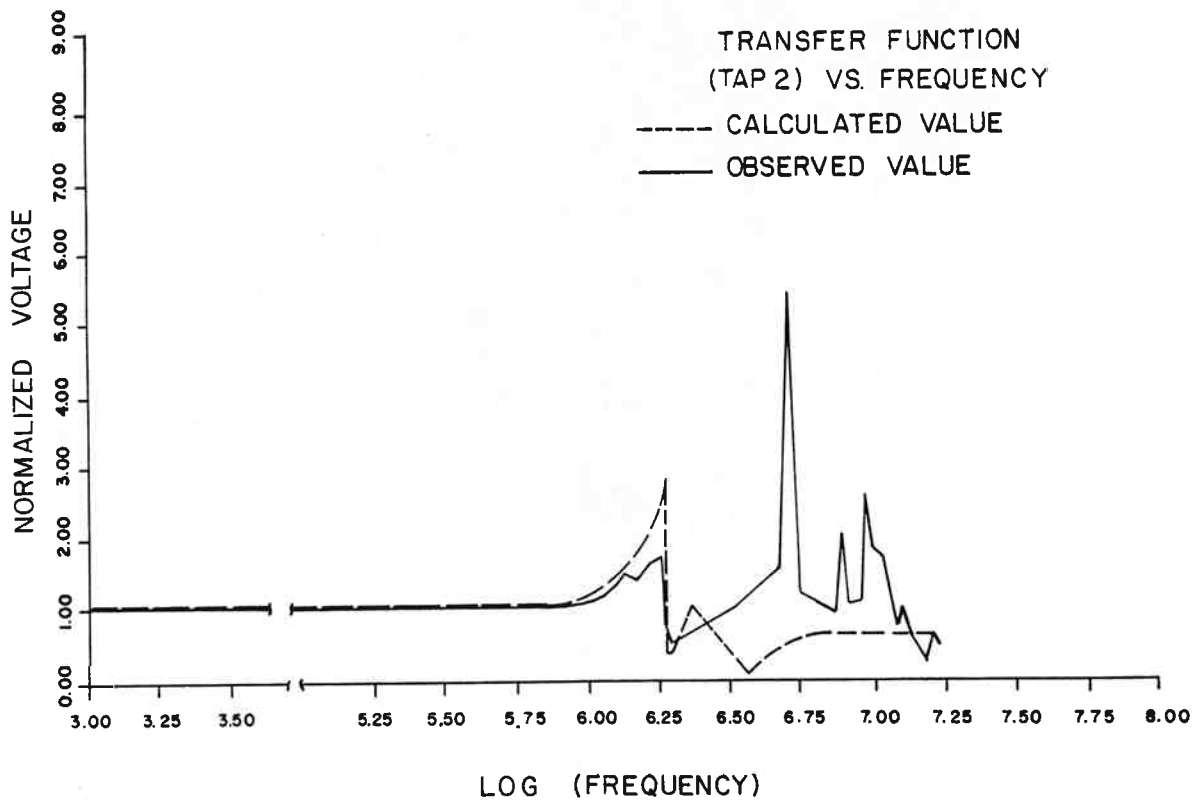


Fig. 5. Response in the frequency domain

$$\text{where } \omega = \omega n L_e \left( \frac{C_g L}{1 - \omega^2 L_e^2 C_c L} \right)^{1/2}$$

For certain frequencies given by

$$\omega_{\text{res}} = \frac{(k\pi/nL_e)}{(LC_g + LC_c L_e^2 (k\pi/nL_e)^2)^{1/2}}, \quad k = 1, 2, 3, 4, \dots$$

it is seen that the voltage at certain points along the winding exceeds the applied voltage. This situation is similar to a resonating L-C circuit, and hence these frequencies will be referred to as resonant frequencies.

The dashed line in Fig. 4 is the graphical representation of Eq. 2 at a resonant frequency. It is seen that sharp potential gradients exist at various points along the winding which could result in the breakdown of interturn insulation.

There are an infinite number of resonant frequencies for different values of the integer  $k$ . It is interesting to note that the sequence of resonant frequencies converges to a single frequency given by

$$\lim_{k \rightarrow \infty} \omega_{\text{res}} = \omega_{\text{cr}} = \frac{1}{L_e \sqrt{LC_c}}$$

The solid line in Fig. 5 is the graphical representation of Eq. 3 for  $\omega > \omega_{\text{cr}}$ . Beyond  $\omega = \omega_{\text{cr}}$ , the poten-

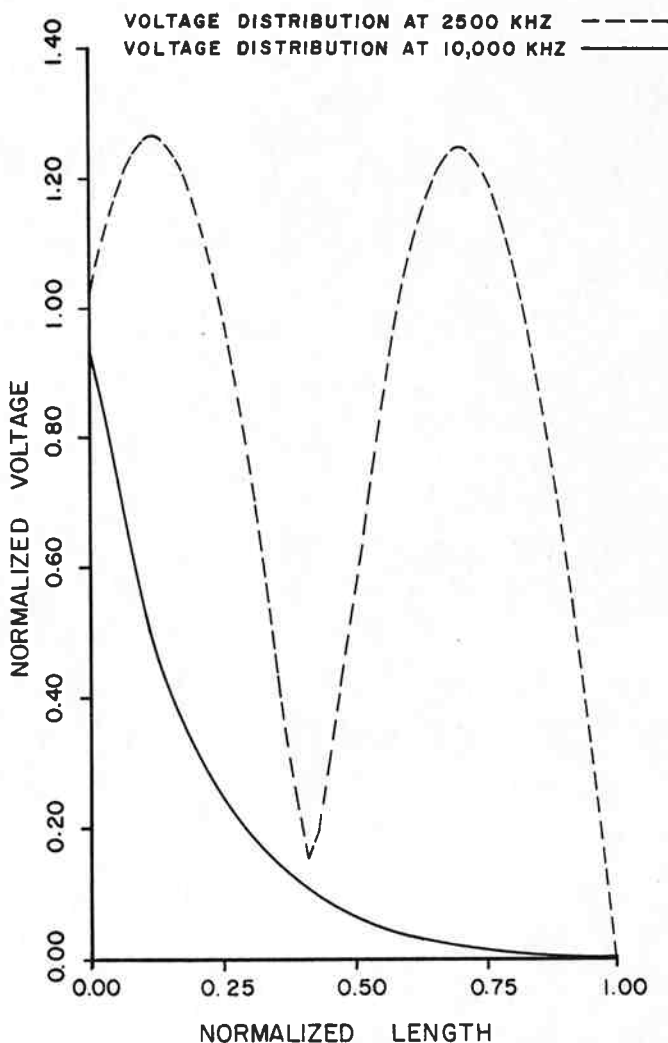


Fig. 6. Voltage distributions for subcritical and supercritical frequencies

tial gradient becomes steeper near the first few turns, until at very high frequencies the voltage distribution is invariant with frequency and depends only on the ratio  $C_g/C_c$ .

A graph of the observed voltage at a particular point on the winding normalized to the magnitude of the applied voltage against frequency is shown in Fig. 6. Observed as well as predicted values are shown, indicating a good match up to 3 MHz.

### Conclusions

From the steady state A-C analysis, we can conclude that the mathematical model is valid up to about 3 MHz. High voltage gradients may exist anywhere along the winding if it is excited at one of the resonant frequencies. At extremely high frequencies, the voltage distribution is similar to the one in response to a step voltage with high potential gradients near the end turns.

### References

1. Ruedenberg, R., "Performance of Travelling Waves in Coils and Windings," *Trans. AIEE*, **59** (1940), 1031-1040.
2. Greenwood, A., *Electrical Transients in Power Systems*, Wiley-Interscience (New York) 1971, 544 p.
3. Bewley, L. V., *Travelling Waves in Transmission Systems*, 2nd ed., Wiley (New York) 1951, 543 p.